Research Square

Preprints are preliminary reports that have not undergone peer review.
They should not be considered conclusive, used to inform clinical practice,
or referenced by the media as validated information.

Cardiac Activity Impacts Cortical Motor Excitability

Esra Al (esraal@cbs.mpg.de)
Max Planck Institute for Human Cognitive and Brain Sciences https://orcid.org/0000-0002-0582-4231

Tilman Stephani
Max Planck Institute for Human Cognitive and Brain Sciences https://orcid.org/0000-0003-3323-3874

Melina Engelhardt
Charité – Universitätsmedizin Berlin

Arno Villringer
Max Planck Institute for Human Cognitive and Brain Sciences

Vadim Nikulin
Max Planck Institute for Human Cognitive and Brain Sciences

Article

Keywords: cognition, somatosensory perception, cardiac cycle

Posted Date: November 9th, 2021

DOI: https://doi.org/10.21203/rs.3.rs-1023617/v1

License: This work is licensed under a Creative Commons Attribution 4.0 International License.
Read Full License

Cardiac Activity Impacts Cortical Motor Excitability

Esra Al[a,b,c], Tilman Stephani[a,f], Melina Engelhardt[d,e], Arno Villringer,[a,b,c], Vadim N. Nikulin[a,g]

a- Department of Neurology, Max Planck Institute for Human Cognitive and Brain Sciences, 04103 Leipzig, Germany

b- MindBrainBody Institute, Berlin School of Mind and Brain, Humboldt-Universität zu Berlin, 10099 Berlin, Germany

c- Center for Stroke Research Berlin (CSB), Charité – Universitätsmedizin Berlin, 10117 Berlin, Germany

d- Charité – Universitätsmedizin Berlin, Klinik für Neurochirurgie, 10117 Berlin, Germany

e- Charité – Universitätsmedizin Berlin, Einstein Center for Neurosciences, 10117 Berlin, Germany

f- International Max Planck Research School NeuroCom, 04103 Leipzig, Germany

g- Institute of Cognitive Neuroscience, National Research University Higher School of Economics, 101000 Moscow, Russia

Correspondence should be addressed to E.A.: esraal@cbs.mpg.de

Abstract

Human cognition and action can be influenced by internal bodily processes such as heartbeats. For instance, somatosensory perception is impaired both during the systolic phase of the cardiac cycle and when heartbeats evoke stronger cortical responses. Here, we test whether these cardiac effects originate from overall changes in cortical excitability. Cortical and corticospinal excitability were assessed using electroencephalographic and electromyographic responses to transcranial magnetic stimulation while concurrently monitoring cardiac activity with electrocardiography. Cortical and corticospinal excitability were found to be highest during systole and following stronger cortical responses to heartbeats. Furthermore, in a motor task, hand-muscle activity and the associated desynchronization of sensorimotor oscillations were stronger during systole. These results suggest that systolic cardiac signals have a facilitatory effect on motor excitability – in contrast to sensory attenuation that was previously reported for somatosensory perception. Thus, distinct time windows may exist across the cardiac cycle that either optimize perception or action.

Introduction

How we perceive and engage with the world is influenced by the dynamic relationship between the brain and the rest of the body including respiratory, digestive, and cardiac systems[1–5]. For example, cardiac activity has been found to influence visual and auditory perception[6–8]. In the domain of somatosensation and pain, perception and neural processing of stimuli have been reported to decrease during the systolic compared to the diastolic phase of the cardiac cycle[9–12]. An overall systolic dampening of cortical processes was suggested to be due to baroreceptor activation during systole[13]. However, for muscle movements, a facilitatory effect of systole has been observed[14–17]. Specifically, saccades, microsaccades, self-initiated movements, and gun shooting occur more often during systole[14–17]. Furthermore, stronger neural responses to heartbeats, i.e., heartbeat-evoked potentials, are followed by increases in visual perception and decreases in somatosensory detection[10,12,18]. It is therefore established that cardiac activity interacts with both perception and action. What remains unknown are the underlying mechanisms of these effects.

One possibility is that cardiac activity exerts its effects through alterations of neuronal excitability in different parts of the brain. A few previous studies have investigated this hypothesis using transcranial magnetic stimulation (TMS) over the primary motor cortex, which induces motor-evoked potentials as an indicator of corticospinal excitability. No cardiac cycle effects were observed on excitability levels[19–21]. However, there are several possible methodological reasons for the null results. The examination of excitability was limited to specific time intervals, rather than across the entire cardiac cycle. Further, individual brain anatomy was not taken into consideration. Lastly, these previous studies only included peripheral measures of corticospinal excitability, without concurrent cortical recordings such as electroencephalography (EEG).

In the present study, we systemically examine whether cortical and corticospinal excitability change across the entire cardiac cycle, and whether they interact with heartbeat-evoked potentials. Neuro-navigated TMS was used in combination with multichannel EEG, in order to comprehensively investigate both cortical and peripheral TMS-evoked responses. If systolic activity attenuates motor excitability, TMS pulses during systole would be expected to produce weaker motor-evoked potentials in the hand muscle and weaker TMS-evoked

potentials in the motor cortex Alternatively, if observations of motor facilitation during systole are correct[14–17], stronger MEPs and TMS-evoked potentials should be observed. Supporting this latter hypothesis, we found that both peripheral and central TMS-evoked potentials were in fact higher during systole. Moreover, stronger heartbeat-evoked potentials preceded increases in excitability. In line with these findings, hand-muscle activity and associated desynchronization of sensorimotor oscillations in a motor pinch task were strongest during the systolic heart phase. Taken together, our results reveal that there is a faciliatory effect of systolic activity on motor excitability, possibly connected with an optimal window for action initiation during the cardiac cycle.

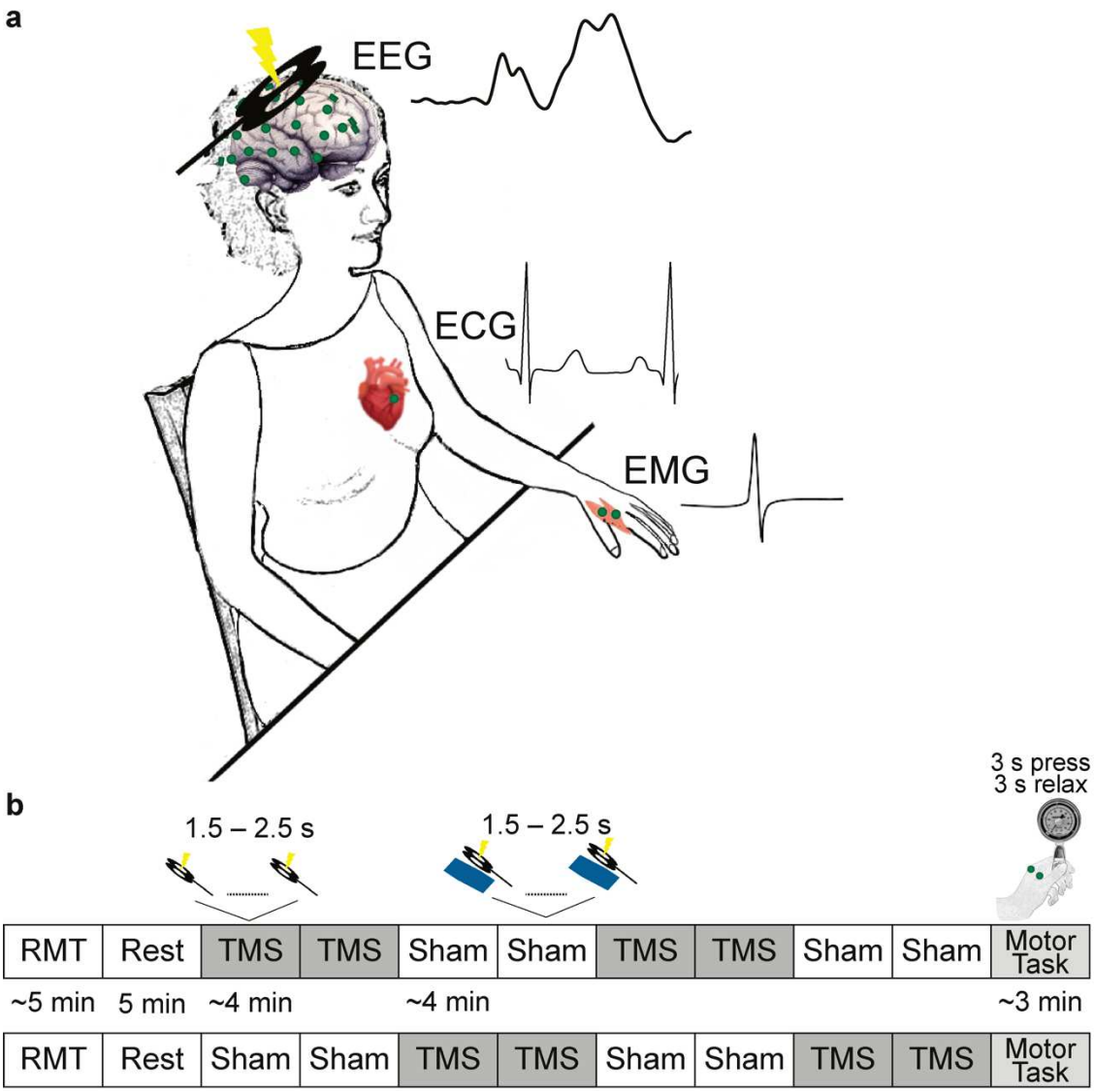

Figure 1. Experimental Paradigm. (**a**) TMS was applied over the right primary motor cortex of the subjects. The motor response to TMS in their left hand, i.e., motor-evoked potential (MEP), was measured by bipolar

electromyography (EMG). Their cortical responses to TMS, the TMS-evoked potential (TEP), as well as to heartbeats, the heartbeat-evoked potential (HEP), were measured using multichannel electroencephalography (EEG). The heart activity was recorded via electrocardiography (ECG). (**b**) After determining the individual resting motor threshold (RMT), subjects underwent a resting-state EEG measurement. Thereafter, 416 single TMS pulses with an intensity of 120% of the RMT were applied in four blocks. There were also four blocks of sham conditions, in which a plastic block was placed between the TMS coil and the head of the subject. The pairs of real and sham TMS blocks were randomized across the subjects. At the end of the TMS blocks, participants performed a motor pinch task. In this task, they were instructed to squeeze a pinch gauge with their left thumb against the index finger while a red circle was presented in the middle of the monitor. When the circle became green, they relaxed their fingers. In this order, subjects performed thirty trials.

Results

Motor-evoked potentials change across the cardiac cycle

To test whether the cardiac phase influences corticospinal excitability, we stimulated the right primary motor area with TMS across the cardiac cycle and recorded motor-evoked potentials (MEPs) of the first dorsal interosseus muscle in the left hand in thirty-six participants (**Fig. 1**). Consistent with the notion of corticospinal excitability changes across the cardiac cycle, MEP amplitudes were significantly higher during systole (mean=1003 µV) relative to diastole (mean=988 µV, $t_{35} = -2.21$, $p = 0.03$; **Fig 2**).

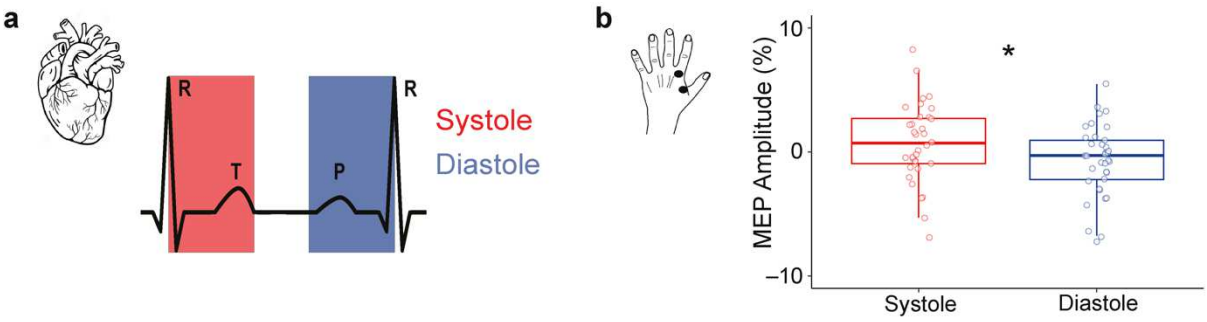

Figure 2. Changes in corticospinal excitability depending on the timing of TMS application across the cardiac cycle. (**a**) Schematic of the cardiac cycle. The systolic phase (indicated in red) starts with the R peak and reflects the ventricular contraction of the heart (leading to blood ejection), whereas the diastolic phase (indicated in blue) represents the relaxation phase during which the heart refills with blood. (**b**) Normalized MEP amplitudes of the first dorsal interosseus muscle in the left hand are higher in response to TMS stimulation during systole (red) compared to diastole (blue). *$p<0.05$

106 **TMS-evoked potentials vary across the cardiac cycle**

107 In addition to corticospinal excitability, we also systematically tested the changes of cortical
108 excitability between the systole and diastole phases of the cardiac cycle using EEG. Cortical
109 excitability was probed by early TMS-evoked potentials (TEPs; 15 - 60 ms post-TMS) measured
110 from a cluster of electrodes (C4, CP4, C6, CP6) over the right motor cortex (hotspot). TEP
111 amplitudes between 22 to 60 ms following the TMS stimulation were stronger during systole
112 as compared to diastole (cluster-based permutation *t*-test, $p_{cluster} = 0.01$; **Fig. 3a**). To test
113 whether these results were indeed related to neural activity of the cortex, rather than
114 reflecting TMS- and cardiac-artifacts, we contrasted them with stimulus-locked EEG signals of
115 the sham TMS condition. A cluster-based permutation test did not reveal any significant
116 difference in TEPs in response to sham TMS during systole and diastole ($p_{cluster} = 0.2$, **Fig. 3b**).
117 Furthermore, to account for physiological and stimulation artifacts, TEPs during sham were
118 subtracted from those in the real TMS condition. The TEP difference was significantly higher
119 between 24 to 60 ms during systole relative to diastole ($p_{cluster} = 0.01$, **Fig. 3c**). The
120 corresponding neural sources of the TEP difference between systole and diastole were
121 observed to be maximal around the right primary motor cortex (**Fig. 3d**).

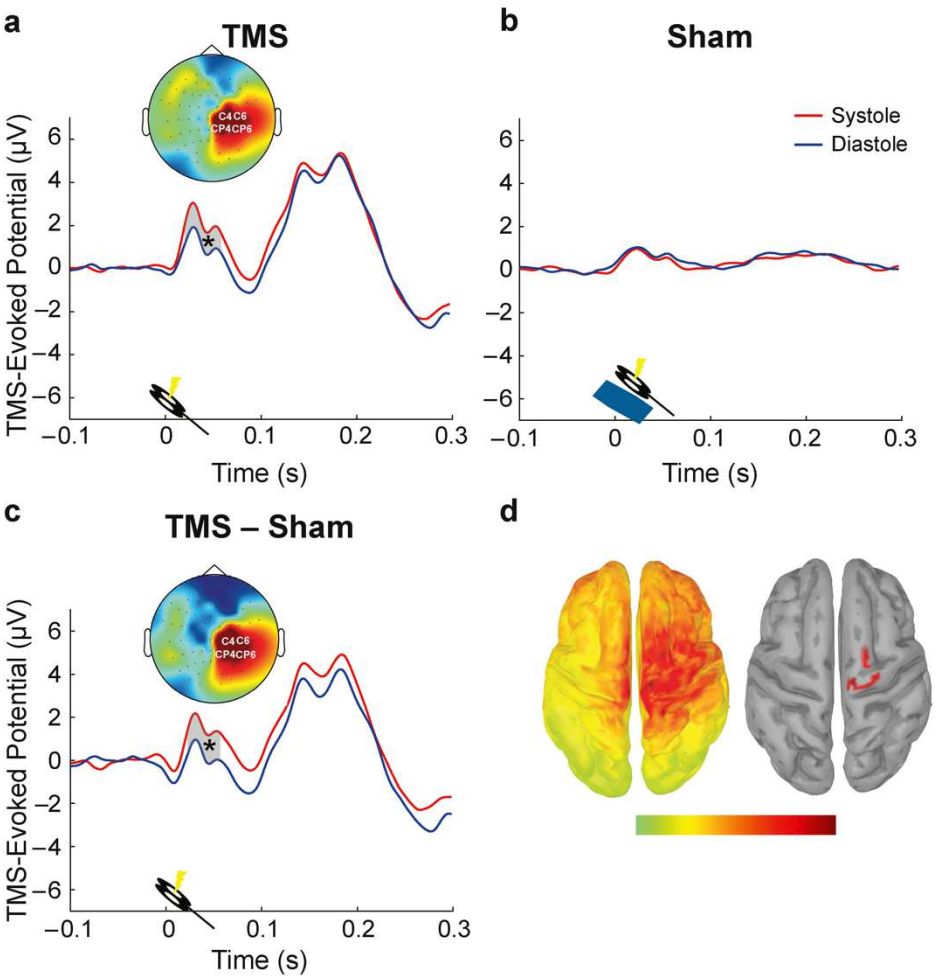

Figure 3. Changes in cortical excitability across the cardiac cycle. (**a**) TMS-evoked potentials (TEPs), in response to TMS stimulation, at the electrodes closest to the motor hotspot (C4; CP4; C6; CP6). Early TEPs were significantly higher during systole as compared to diastole between 22 – 60 ms in motor areas. The contrast between systole and diastole in this time window is shown in the topography plot. (**b**) Same as a, however for the sham TMS condition. No significant differences between systole and diastole were observed here. (**c**) The difference-curve between real TMS and sham for systole and diastole (corrected TEP contrast). After accounting for the TMS and physiological artifacts, TEPs during systole and diastole were significantly different between 24 – 60 ms. (**d**) (left) The source reconstruction of the corrected TEP contrast between systole and diastole between 24 – 60 ms. (right) Same as the left figure but displaying the strongest generators only (thresholded at 85% of the maximum activity and clusters sizes of at least five vertices).

Muscle-related peripheral and central activity fluctuates across the cardiac cycle

In a follow-up motor pinch task, we then investigated whether higher motor excitability during systole was associated with an increase in the actual muscle activity during systole. For this purpose, we recorded EMG, EEG, and ECG activity while subjects were performing a

motor pinch task, where they were asked to pinch a dynamometer with their index finger and thumb (**Fig. 4a**). To estimate peripheral muscle force, we calculated the linear envelope of EMG activity when subjects initiated the pinch during systole and diastole. Cluster statistics revealed a significant increase in the normalized EMG envelope from 220 to 522 ms after the onset of the pinch, during systole compared to diastole ($p_{cluster,}$= 0.01, **Fig. 4a**). To test whether this finding might have been related to blood circulation-related changes in the fingers, we sampled systolic and diastolic EMG activity during the resting state condition. This analysis did not reveal any significant difference in the resting EMG envelope between systole and diastole (no significant clusters were found). This indicates that there was no influence of cardiac-related artifacts on the EMG signal across the cardiac cycle.

Following the analysis of the muscle activity in the periphery, we also tested whether sensorimotor oscillations (in the range of 8 – 30 Hz) in the motor areas desynchronize differently following the initiation of the pinch during systole and diastole. This analysis demonstrated that the desynchronization of sensorimotor oscillations in the range of 8 – 25 Hz was stronger between 0 and 726 ms following pinch onset during systole as compared to diastole ($p_{cluster}$ = 0.01, **Fig. 4b, c**). To investigate whether this finding was influenced by cardiac-related artifacts, we again sampled systolic and diastolic windows during the resting state and tested the differences in sensorimotor oscillations between systole and diastole. Also, in this control analysis, no significant differences were found ($p_{cluster}$ = 0.12). Thus, these results indicate that both peripheral muscle activity and its central correlates are stronger when the movement starts during systole as compared to diastole.

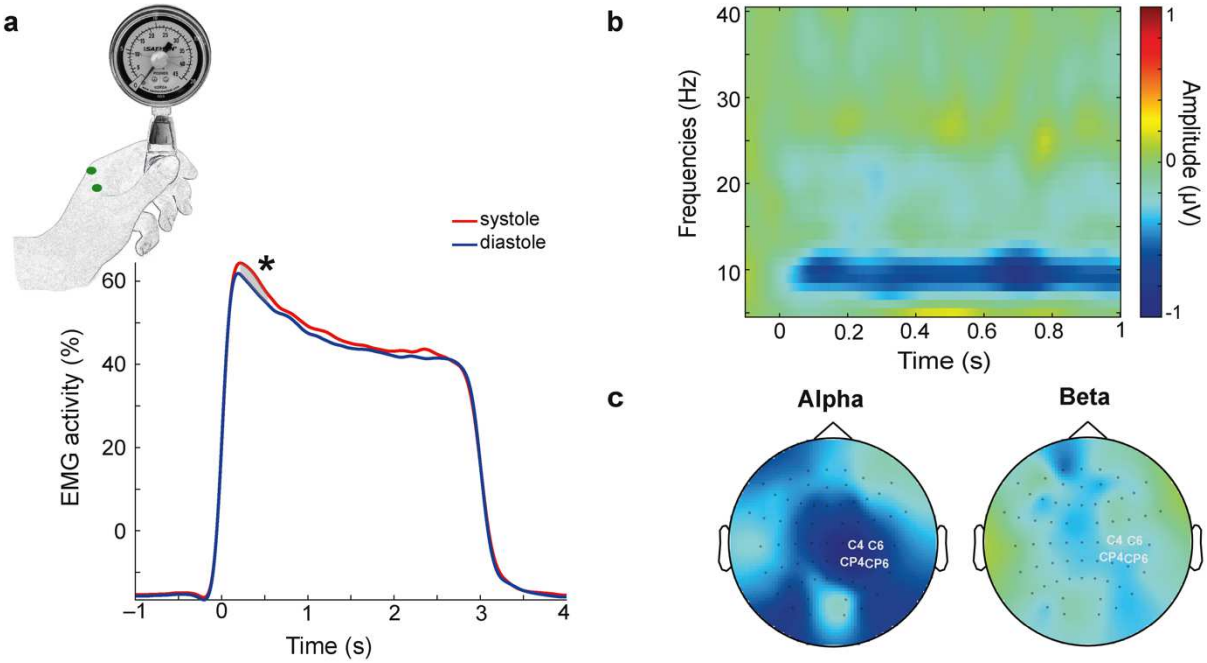

Figure 4. Fluctuations of muscle-related activity depending on the pinch onset across the cardiac cycle during a motor pinch task. (**a**) Muscle force, measured by the normalized linear envelope of EMG activity, in the left hand, was significantly higher from 220 to 522 ms following pinch onset (at 0 ms) during systole compared to diastole. (**b**) Similarly, systolic and diastolic sensorimotor oscillations were analyzed in the range of 8 – 30 Hz in the sensorimotor electrodes to quantify event-related desynchronization following the muscle activation. Cluster statistics revealed that when subjects started the pinch during systole, the desynchronization of sensorimotor oscillations was higher in the frequency range of 8 – 25 Hz between 0 and 726 ms following pinch onset. The raster plot shows the contrast between systole and diastole. (**c**) The topography of this significant contrast is also shown individually for alpha (8 – 13 Hz) and beta (14 – 25 Hz) sensorimotor oscillations.

Heart rate changes depending on the timing of TMS across the cardiac cycle

We further investigated the changes in the heart rate in response to TMS stimulation during systole and diastole across time (pre-TMS, TMS, post-TMS). The analysis showed a main effect of time ($F_{2, 70} = 23.11$, $p = 2{\cdot}10^{-8}$) and an interaction of time and cardiac phase ($F_{2, 70} = 10.30$, $p = 1{\cdot}10^{-4}$) on heart rate. Comparison of heartbeat intervals preceding TMS and concurrent with TMS revealed a significant cardiac deceleration when TMS stimulation occurred during systole ($t_{35} = -5.73$, $p = 2{\cdot}10^{-6}$). This was followed by a cardiac acceleration (from TMS to post-TMS; $t_{35} = 8.58$, $p = 4{\cdot}10^{-10}$, **Fig. 5**). No significant changes were observed for stimulations during diastole (from pre-TMS to TMS, $t_{35} = 0.75$, $p = 0.5$ and from TMS to post-TMS, $t_{35} = 0.42$, $p = 0.68$, **Fig. 5**). To control whether these heart rate changes were due to genuine effects of

TMS rather than artifacts (e.g. auditory, somatosensory) induced by TMS application, heart rate across time was adjusted with the heart rate during the sham TMS condition individually for each time interval and cardiac phase. This analysis again showed a similar main effect of time ($F_{2, 70} = 7.42$, $p = 1 \cdot 10^{-3}$) and an interaction of time and cardiac phase ($F_{1.56, 54.64} = 3.88$, $p = 0.03$) on heart rate.

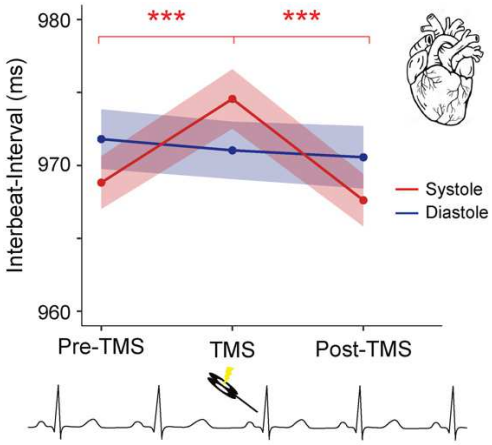

Figure 5. Heart rate changes induced by TMS are influenced by the cardiac cycle. The heart first slowed down and then accelerated when TMS pulses were delivered during systole. No significant differences were observed for stimulations during diastole. Colored bands indicate 95% within-participant confidence intervals[52]. ***$p < 0.0005$

Heartbeat-evoked potentials fluctuate depending on motor excitability levels

Apart from the cardiac phase effects, we examined the relationship between motor excitability and preceding cortical responses to heartbeats, so-called heartbeat-evoked potentials (HEP). For this purpose, we sorted single trials according to their MEP amplitudes and split them into three equal bins for each participant. We then contrasted prestimulus HEP amplitudes for weak and strong MEP levels by using a cluster-based permutation *t*-test in the *296 – 400* ms *post R-peak time window* in the centroparietal electrodes as identified in previous studies[10,12]. HEPs were significantly higher preceding strong in comparison to weak MEP amplitudes, between 304 – 324 ms over the centroparietal electrodes ($p_{cluster} = 0.02$ corrected for multiple comparisons in space and time; **Fig. 6a, b**). To test whether these effects are induced by overall changes in cardiac activity during TMS stimulation, we further tested the differences in HEP activity during TMS stimulation and resting-state condition (without TMS stimulation). No significant differences in HEP amplitudes during TMS and resting-state were observed (no clusters were found; **Supplementary Fig. 2**).

Heart rate fluctuates depending on motor excitability levels

We furthermore investigated the effect of motor excitability on heart rates. For this purpose, we tested the relationship between interbeat-intervals, that is, the duration between two consecutive heartbeats, and MEP amplitudes. Increases in MEP amplitudes correlated with decreases of the interbeat-intervals (repeated measures correlation, $r = -0.48$, $p = 2 \cdot 10^{-5}$, **Fig. 6c**). In other words, as motor excitability increased, the heartbeats became faster.

As a control analysis, we also tested whether heart rates differed between the resting-state condition and during TMS application. No significant differences in heart rate were observed here ($t_{35} = 0.28$, $p = 0.78$).

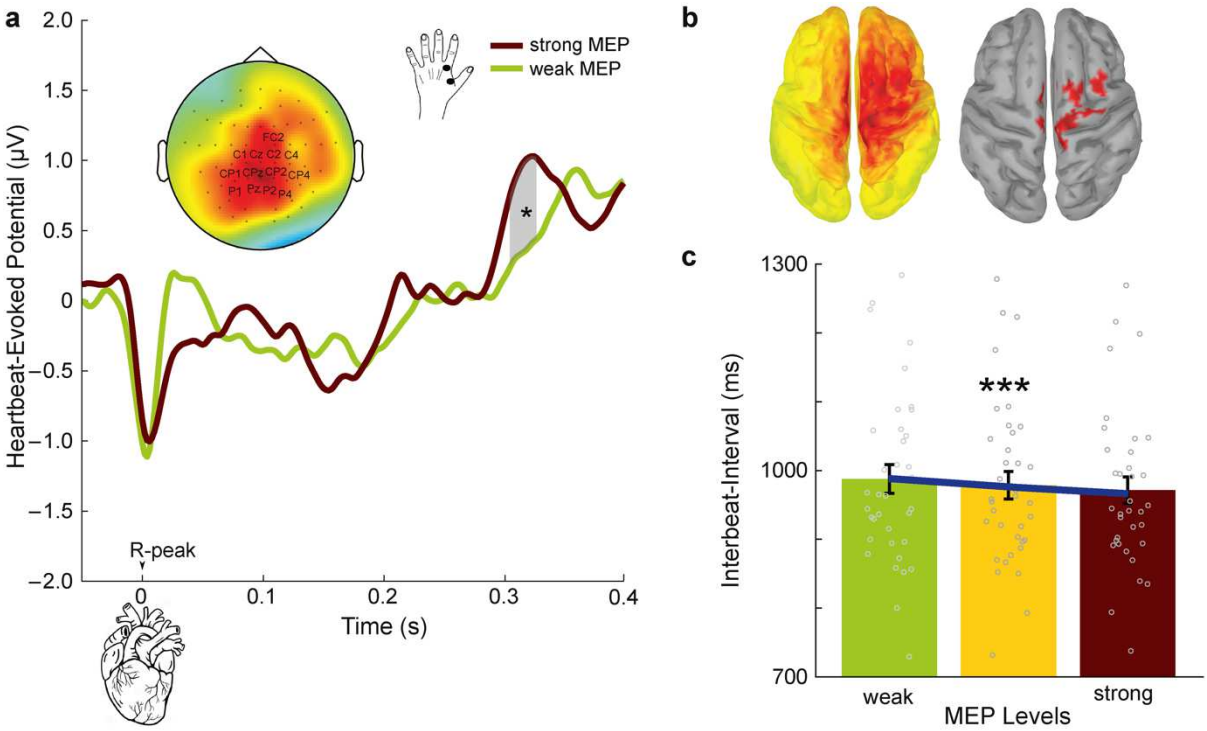

Figure 6. The cortical responses to heartbeats, heartbeat-evoked potentials (HEPs), preceding changes in the strength of motor excitability. (**a**) To assess relationship between HEPs and motor excitability, single trials were sorted according to MEP amplitudes and split into three equal bins for each subject. HEP amplitudes between 304–328 ms following the R-peak (the highlighted gray area) were higher preceding strong compared to weak motor-evoked potentials (MEPs) across the centroparietal electrodes. The topography contrast represents HEP amplitude difference preceding strong versus weak MEPs between 304–328 ms. (**b**) (left) The neural sources of HEP differences preceding strong and weak MEPs are visualized. (right) Same as the left figure but displaying the strongest generators only (thresholded at 85% of the maximum activity and clusters sizes of at least five vertices). (**c**) Interbeat-interval became shorter

227 for stronger MEP amplitudes. In other words, subjects' motor excitability increased as their heart beat
228 faster. *$p<0.05$, ***$p<0.0005$.
229
230 **Control analyses for movement of cortex across the cardiac cycle**
231 Next, we investigated whether our findings of larger motor excitability during systole might
232 have been related to the displacement of the cortex due to blood influx and efflux (as a result
233 of cardiac activity). The mechanical displacement of the cortex follows an inverse u-shaped
234 pattern across the cardiac cycle, rather than a linear relationship, and it reaches its maximum
235 at 450-500 ms after the R-peak[22]. To observe whether MEP amplitudes followed a similar
236 pattern across the cardiac cycle, we first visualized MEP amplitudes across 50ms bins
237 following the previous R-peak (**Supplementary Fig. 1**). This demonstrated that MEPs were
238 maximal during the first 50 ms and gradually decreased across the cardiac cycle. To
239 statistically test the relationship between MEP amplitudes and the distance from the previous
240 heartbeat, linear-mixed-effects model regressions were fit on the single-trial level. The linear
241 regression that included the cardiac distance (MEP ~ distance + (1 | subject)) explained the
242 empirical data better than the null model, i.e., a model with no relationship assumed (MEP ~
243 (1 | subject); $\chi^2 = 4.67$, $p = 0.03$). Crucially, this linear model also showed a better fit than a
244 second-degree polynomial model (MEP ~ distance + distance^2+ (1 | subject), $\chi^2 = 0.34$,
245 $p = 0.6$). This result indicates that the changes in MEP amplitudes do not follow a u-shaped
246 pattern across the cardiac cycle and are thus not likely to be explained by the displacement
247 of the cortex due to blood influx or efflux.
248
249 **Discussion**
250 Using simultaneous recordings of cortical, cardiac, and muscle activity with EEG, ECG, and
251 EMG in response to TMS stimulation, we found that cardiac signals and their neural
252 processing were associated with changes of motor excitability. More specifically,
253 corticospinal excitability, probed by motor-evoked potentials in the FDI muscle of the left
254 hand, was significantly higher when TMS coincided with the systolic as compared to the
255 diastolic phase of the cardiac cycle. In line with changes in corticospinal excitability, we
256 further showed that cortical excitability, as measured by TMS-evoked potentials in the motor
257 cortex, was stronger during systole. Moreover, consistent with this finding, in the motor pinch
258 task we observed that muscle activity and desynchronization of sensorimotor oscillations

were stronger following muscle contractions during systole (as compared to diastole). Furthermore, we observed significant modulations of heart rate when TMS was presented during systole, while diastolic stimulations did not trigger any significant changes in heart rate. In addition to cardiac timing effects, increases in cortical responses to heartbeats, as measured by heartbeat-evoked potentials, predicted stronger corticospinal excitability, which also correlated positively with heart rate. These results are unlikely to reflect stimulation artifacts since both heartbeat-evoked potentials and heart rates were comparable between resting-state and TMS conditions.

Methodological differences are likely to explain the absence of cardiac modulation of motor excitability in previous TMS studies[19–21]. In those studies, time resolution across the cardiac cycle was rather limited. Unlike our study, TMS stimulations were not presented throughout the entire cardiac cycle, rather they were presented up to 400 or 600 ms after the heartbeats and at specific time points (e.g., 100 ms after R-peak). Since our study revealed a linear decrease in motor excitability throughout the cardiac cycle, previous studies might not have been able to sample the decrease towards the end of the cardiac cycle. Furthermore, combining a neuro-navigational system with individual brain scans might have provided us with a higher spatial specificity for the stimulation location, in comparison to previous studies. In addition, our study had the advantage of a larger sample size and trial numbers, which contributed to higher statistical power to detect the cardiac-cycle effects on motor excitability [19–21]. Finally, we also used concurrent EEG recordings in addition to MEPs, which allowed us to directly investigate cortical effects.

Cardiac cycle effects on motor excitability are consistent with previous findings of increased frequency of muscle movement during systole as compared to diastole[14–17]. Here, we showed that TMS during systole is associated with higher corticospinal and cortical excitability in motor areas. Thus, motor-related activity seems to be facilitated during systole. This in turn may also explain why eye movements[15,16], e.g., (micro)saccades, and voluntary hand movements[17], e.g., firing a gun, have been found to occur more often during systole. One could also argue that the effects we found were merely due to the fact that the distance of the brain to the skull (and thus the TMS coil) changes due to fluctuations in intracranial pressure throughout the cardiac cycle[23]. This, in turn, should affect the induced electric field

291 from TMS. However, our control analyses did not support this argument. More specifically,
292 the movement of the brain follows an inverse u-shaped pattern across the cardiac cycle and
293 reaches a maximal distance at about 450-500 ms after the previous heartbeat[22]. If the cortical
294 movement across the cardiac cycle was responsible for the cardiac phase effects, then MEPs
295 would be expected to follow a similar pattern across the cardiac cycle. However, MEP
296 amplitudes decreased rather linearly across the cardiac cycle, differently than effects that
297 would be expected due to cortical movement. This result indicates that the changes in MEP
298 amplitudes are not likely to be explained by the displacement of the cortex across the cardiac
299 cycle. Another possible artifact, which can influence the amplitude of the evoked activity, are
300 muscle-related far-fields from the cardiac activity (typically referred to as "cardiac artifacts"
301 in the EEG). To control for those, we included a sham condition, in which auditory, tactile, and
302 cardiac artifacts were comparable. After the correction of real TMS recordings with the sham
303 condition, cortical excitability was still significantly higher during systole as compared to
304 diastole. Overall, these results suggest that motor excitability is higher during systole,
305 suggesting an optimal window for motor activity across the cardiac cycle.
306
307 The cardiac cycle was also observed to affect muscle activity in a motor task, where subjects
308 were asked to pinch and release a dynamometer with their left index finger and thumb. When
309 the pinch was initiated during systole, compared to diastole, muscle activity was transiently
310 stronger. In addition to the peripheral activity, we analyzed cardiac effects on the central
311 neural activity during the motor task. Previous studies have shown that following muscle
312 contractions, sensorimotor oscillations desynchronize in the motor regions, which is reflected
313 as an amplitude decrease in the alpha and beta range[24,25]. Here, we found that this
314 desynchronization transiently increased when the pinch was initiated during systole.
315 Furthermore, these cardiac effects on the muscle-related activity are not likely due to cardiac
316 artifacts, since no significant differences in muscle and neural activity were observed across
317 the cardiac cycle while subjects were resting. Overall, these findings suggest that muscle
318 activity is stronger when movement is initiated during systole due to an increase in motor
319 excitability.
320
321 The increased motor excitability during systole seems to be at odds with the previously shown
322 cardiac effects on perception. For example, we recently demonstrated that somatosensory

323 percepts and their neural processing are attenuated during systole[10,12]. We explained these
324 findings by an interoceptive predictive coding account, which postulates that rhythmic
325 cardiac signals are predicted and suppressed from entering conscious perception. This
326 mechanism was suggested to additionally inhibit the perception of coincident weak external
327 stimuli[10,12]. Furthermore, this suppression of non-salient sensory stimuli was suggested to
328 lead to a greater uncertainty about threatening factors in the environment[26]. To compensate
329 for it, the organism might increase expectation for a "risk" and use its limited resources for a
330 "flight or fight" motor response, which can be potentially mediated by increased
331 baroreceptor activity during systole. Therefore, it is possible that the increased motor activity
332 during systole might provide a survival advantage. Hence, this would suggest that there are
333 different optimal windows for action and perception throughout the cardiac cycle. This idea
334 also fits well with previous studies on "sensory gating", in which somatosensory perception
335 and evoked potentials were shown to be attenuated during movement[27–29]. Given that action
336 has an inhibitory effect on perception, it is plausible that systolic facilitation of action is indeed
337 consistent with inhibition of perception during the systolic phase of the cardiac cycle.
338
339 Cortical excitability changes have been associated previously with epilepsy, chronic insomnia,
340 disorders of consciousness, stroke, and depression. To counterbalance these abnormalities in
341 cortical excitability, the therapeutic applications of TMS have been introduced, e.g., for
342 treating depression[30] or facilitating recovery during neurorehabilitation[31]. Our results on
343 cardiac modulations of cortical excitability raise some important questions for these clinical
344 populations. For example, it remains unknown whether cortical excitability over the cardiac
345 cycle is modulated in those pathological conditions. Furthermore, our observation that TMS
346 induces changes of the heart rate during systole, i.e., when the cortical processing of
347 heartbeats occurs, but not during diastole, can have important implications for clinical use of
348 TMS. When the changes in heart rate of patients during TMS application are a clinical concern,
349 then our results indicate that stimulation during diastole can prevent these unwanted
350 changes. In contrast, synchronization of TMS with systolic activity might be relevant for
351 treatment of clinical subgroups, such as depression, which is often associated with decreased
352 heart rate variability and increased heart rate[32–34]. Our results, therefore, suggest that
353 application of TMS during systole or diastole might be helpful to optimize clinical protocols,
354 which should be addressed in future studies.

Another effect of cardiac activity on motor excitability was found on the cortical level. We observed that heartbeat-evoked potentials (HEPs), during systole, showed higher positivity over centroparietal electrodes between 304 and 328 ms preceding strong as compared to weak corticospinal excitability (as measured by TMS-induced MEPs). These results again diverge from our previous results on somatosensory perception, in which we observed higher HEPs preceding attenuated somatosensory processing. We previously explained increases in HEPs as a result of an attentional switch from the external world to internal bodily signals, such as heartbeats [10]. This was further supported by higher HEP amplitudes when subjects were resting compared to engaging in an external task[12]. If internal attention levels changed in the current study during the TMS condition compared to rest, we would expect lower HEPs during the TMS condition. However, in the current study, there was no significant change in HEPs during the TMS application in comparison to the resting state of the subjects. This was probably related to the absence of an external task during the TMS condition. Another factor, which can positively influence HEP amplitude, is arousal[35]. Increases in arousal are also known to increase motor excitability[36] as well as heart rate[1,37]. Supporting a possible involvement of arousal in our study, we observed that heart rate became higher as motor excitability increased. Therefore, we suggest that increases in arousal might be responsible for increases in HEP amplitudes for stronger motor excitability. It is also possible that since this analysis involves HEPs and MEPs, which were close in time, there was a similar cortical state for both responses due to intrinsic neuronal dynamics, thus explaining the covariation between them.

In conclusion, our study provides novel insights into the regulation of cortical and corticospinal excitability by cardiac function in healthy individuals. Together, these findings strongly suggest that systolic cardiac activity and its cortical processing have faciliatory effects on motor excitability, in contrast to the previous findings on somatosensory perception. Thus, we propose that optimal windows for action and perception may differ across the cardiac cycle. Furthermore, these results may contribute to the development of novel stimulation protocols and promote a better understanding of the interplay between brain dynamics and bodily states in both health and disease.

385 **Methods**

386 Participants

387 37 healthy volunteers participated in the experiments after giving written informed consent.
388 All protocols were approved by the Ethical Committee of the University of Leipzig's Medical
389 Faculty (Ethics no: 179/19). One subject was excluded due to failure in the data acquisition.
390 In the remaining 36 subjects (20 female, age: 27.97 ± 4.13, mean ± SD), only one subject was
391 left- handed as assessed using the Edinburgh Handedness Inventory [38].

392

393 TMS setup and neuronavigation

394 The experiment included 4 blocks of sham and 4 blocks of real TMS stimulations. Participants
395 were seated in a comfortable armchair and asked to keep their eyes on a fixation point on a
396 wall in front of them throughout the measurements. TMS pulses were delivered through a
397 Magstim 200 Bistim stimulator (Magstim Company Ltd, Whitland, UK) connected to a figure-
398 of-eight coil (Magstim "D70 Alpha Coil"). The coil was positioned at an angle of 45° with
399 respect to the sagittal direction. Structural T1 weighted MRIs of the subjects were used with
400 the TMS neuronavigation system (Localite GmbH, Bonn, Germany) to identify the hotspot of
401 the left first dorsal interosseous muscle (FDI). Then, the resting motor threshold was
402 determined as the lowest TMS intensity at which 5 out of 10 trials yielded a motor response
403 greater than 50 µV (peak-to-peak amplitude). The TMS blocks consisted of 104 trials, i.e., a
404 total of 104 x 8 = 832 stimulations. The neuronavigation system was used to control the coil
405 position over the hotspot during the TMS stimulations. TMS intensity was set to be 20% above
406 the motor threshold at rest (corresponding to 66.58 ± 9.16% of the maximum stimulator
407 output). The interstimulus interval was uniformly randomized between 1.5 and 2.5 seconds.
408 The blocks were presented as pairs of two sham or real TMS and their order were randomized
409 across participants. For the sham TMS condition, we used a custom-manufactured 3.5 cm
410 plastic block between the coil and the participant's head to keep air- and bone-conducted
411 auditory sensations similar to the real TMS[39]. This setup also mimicked a tapping
412 somatosensory sensation associated with the vibration of the TMS coil.

413

414 EEG, ECG and EMG recordings

415 TMS-compatible EEG equipment (NeurOne Tesla, Bittium) was used for recording EEG activity
416 from the scalp. The EEG was acquired with a bandwidth of 0.16-1250 Hz from 62 TMS-

417 compatible c-shaped Ag/AgCl electrodes (EasyCap GmbH, Herrsching, Germany) mounted on
418 an elastic cap and positioned according to the 10–10 International System. POz electrode was
419 used as ground. During the measurements, the EEG signal was referenced to an electrode
420 placed on the left mastoid. Additionally, a right-mastoid electrode was recorded so that EEG
421 data could be re-referenced to the average of both mastoid electrodes offline. The signal was
422 digitized at a sampling rate of 5 kHz. Skin/electrode impedance was maintained below 5 kΩ.
423 EEG electrode positions were also coregistered with the structural MRIs using the
424 neuronavigation system. To reduce auditory response artifacts in the EEG induced by coil
425 clicks, participants wore earplugs throughout the experiment. An additional ECG electrode
426 connected to the EEG system was placed under the participant's left breast to record the
427 heart activity. Furthermore, EMG electrodes were attached to the left first dorsal interosseus
428 (FDI) muscle in belly-tendon montage via a bipolar channel connected to the EEG system to
429 record the TMS-induced motor-evoked potentials (MEP). At the beginning of the experiment,
430 EEG and ECG data were acquired during a 5-min eyes-open resting-state measurement.
431
432 Automated Cardiac Phase Classification
433 The fluctuations of motor excitability were tested across the systolic and diastolic phases of
434 the cardiac activity. Systole was defined as the time between the R-peak and the end of the
435 t-wave, which was determined by using a trapezoid area algorithm[10,40]. We then used the
436 duration of systole to define an equal length of diastole at the end of each cardiac cycle. [10] As
437 a result, the average systole (and diastole) length was 351± 21 ms. Before using this
438 automated algorithm, we removed large TMS artifacts on the ECG data by removing -2 to 10
439 ms window around the TMS stimulation and then applied cubic interpolation.
440
441 Motor-Evoked Potentials
442 As an index of corticospinal excitability, motor-evoked potentials (MEPs) were used. Peak-to-
443 peak MEP amplitudes were calculated in the EMG data in the time window of 20 – 40 ms
444 following the TMS stimulation. To investigate possible changes of MEP amplitude across the
445 cardiac cycle, we contrasted the averaged MEP amplitudes between systole and diastole.
446
447

448 TMS-Evoked EEG Potentials

449 EEG data was first segmented between -1400 and 1000 ms around TMS stimulations. Then,
450 the baseline correction was performed using -110 to -10ms prestimulus window. The large
451 amplitude TMS-artifacts between -2 to 8 ms were removed from each trial and then the
452 remaining data segments were concatenated. Then, ICA (round 1) was applied using
453 pop_runica as implemented in EEGLAB, used with the FASTICA algorithm [41]. To remove TMS
454 decay artifacts, the three largest components explaining the variance between -150 to 150
455 ms were removed and other components were forward-projected. After the decay artifact
456 was removed in this way, copies of these datasets were kept. Then, a 4th order Butterworth
457 bandpass filter (0.5-45 Hz) and a 50 Hz notch filter (with a stopband of 45-55 Hz) were applied.
458 A second round of ICA was applied to determine remaining TMS, ocular, muscle and cardiac
459 artifacts. Afterwards, these ICA weights were applied on the copied dataset after the first
460 round of ICA (unfiltered). After artifactual components were removed and the data was
461 forward-projected, we further removed 15 ms post-stimulus window since TMS-evoked
462 artifacts were still present in this time window. We then applied a cubic interpolation (for -2
463 to 15ms window) before applying the same filtering procedure (as described above) to the
464 data. This way we ensured that the TMS artifacts did not smear into the post-stimulus window
465 during the filtering process. Then, data was re-referenced offline to the average of the right
466 and left mastoid signals and down-sampled to 500 Hz (**Fig. 6**).

467

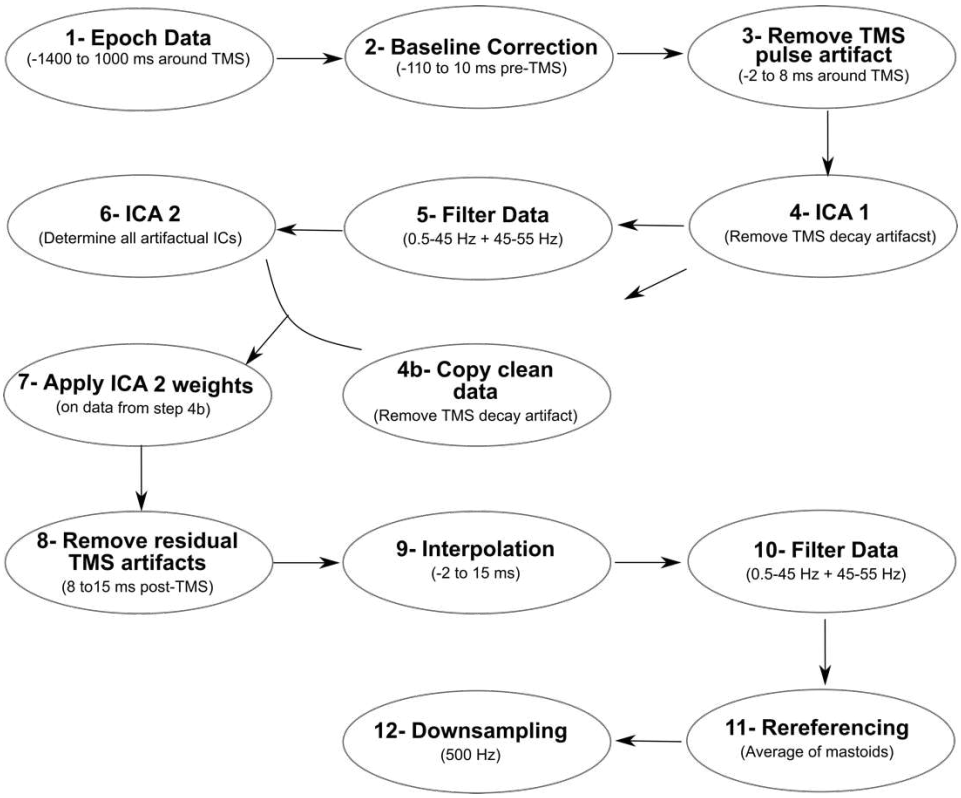

Figure 6. Preprocessing steps of EEG data for cleaning artifacts in the post-TMS window. These steps were followed before calculating TMS-evoked potentials (TEPs).

In further analyses of the TMS-EEG data, we only included trials in which TMS stimulation triggered a motor-evoked potential higher than 50 µV, which yielded on average 412 trials per subject. For the sham TMS condition, we only included trials, in which no evoked motor activity was observed (405 trials on average).

To asses cortical excitability, we focused on early components of TMS-evoked potentials (TEPs) in the first 60 ms following the stimulation since these window indicates the activation of local neuronal populations in the motor cortex[42]. Since the first 15 ms were interpolated, we evaluated TEPs between 15-60 ms in the post-TMS window in a cluster of electrodes over the right primary motor cortex (C4, CP4, C6, CP6).

Cardiac artifact during systole and diastole was estimated during TMS and sham conditions (see Al et al., 2020 for details on the pulse artifact cleaning of the evoked potentials) and subtracted from TMS-evoked potentials during systole and diastole individually.

487 Heartbeat-Evoked Potentials

488 In this analysis, we only included trials in which TMS stimulation was at least 400 ms after the
489 previous R-peak (i.e., during diastole) to keep the heartbeat-evoked potential window free of
490 TMS-related activity. To clean TMS artifacts in the prestimulus window and keep data
491 processing close to our previous work [10,12], some preprocessing steps were altered compared
492 to the steps described above for the post-stimulation analyses: After the second round of ICA,
493 we first calculated each distance between the prestimulus R peaks and TMS events. Then, we
494 shuffled these distances and inserted "mock events" by subtracting them from the latency of
495 TMS stimulations in the dataset. Next, we repeated this shuffling process ten times. Finally,
496 we segmented data between -100 to 400 ms around these mock events. By using an average
497 of these segments, we derived an estimate of the TMS artifact in the time window of the
498 heartbeat-evoked responses per subject.

499

500 We then subtracted this estimation from each heartbeat-evoked potential to remove any
501 potential TMS artifacts.

502

503 Source Analyses

504 The neural sources of the TMS- and heartbeat-evoked potentials were reconstructed with the
505 Brainstorm toolbox [43] using individually measured electrode positions with a TMS neuro-
506 navigation system (Localite GmbH, Bonn, Germany). For every subject, the individual
507 structural T1-weighted MRI images were segmented using Freesurfer
508 (http://surfer.nmr.mgh.harvard.edu/). A 3-shell boundary element model (BEM) was
509 constructed to calculate the lead field matrix with OpenMEEG [44,45]. The lead field matrices
510 were inverted using eLORETA individually for each condition and participant. Individual
511 source data were then projected to the ICBM152 template [46].

512

513 Motor Pinch Task

514 After the TMS sessions, participants performed a pinch motor task. At the beginning of the
515 task, their maximal pinch strength, i.e., maximal voluntary contraction (MVC), was calculated
516 using SAEHAN® Hydraulic Hand Dynamometer Model SH5005 (SAEHAN Corporation, Korea).
517 Participants were asked to squeeze the dynamometer with their left thumb pad against the
518 lateral aspect of the middle phalanx of the left index finger as hard as possible while keeping

519 their elbow in the 90° position. After calculating MVC, participants were asked to apply 30%
520 of this contraction value (corresponding to 3.14 ± 0.88 pounds) when a green circle in the
521 middle of the monitor returned to red. During the presentation of the red circle, which lasted
522 for three seconds, they were asked to keep the contraction. When the circle became green
523 again, they relaxed their hand for three seconds. In this order, subjects performed
524 contractions for thirty trials.
525
526 EMG Envelope
527 To estimate muscle activity during the pinch task, EMG data were analyzed. First, the signal
528 was cleaned from movement-related artifacts and noise with the application of a 4th order
529 Butterworth bandpass filter (10-500 Hz) and a 50 Hz notch filter (with a stopband of 45-55
530 Hz). Afterwards, the envelope of EMG was calculated by first taking the absolute value of the
531 signal ("full-wave rectification") and then applying a low pass filter (2nd order Butterworth, 3
532 Hz) [47]. The resulting EMG linear envelope was normalized by dividing it by the peak muscle
533 activation value during each trial. This was followed by a baseline correction using the -110
534 to -10ms pre-movement EMG signal. Finally, an average of the envelope was calculated when
535 pinch onset coincided with the systolic and diastolic phases of the cardiac cycle per subject.
536
537 Desynchronization of Sensorimotor Oscillations during the Motor Task
538 To investigate the central sensorimotor oscillations following pinch onset during systole and
539 diastole, we also analyzed EEG signals. For this purpose, we first filtered the data with a 4th
540 order Butterworth bandpass (0.5-45 Hz) and a 50 Hz notch filter (with a stopband of 45-55
541 Hz). After cleaning muscular, cardiac, and ocular artifacts through ICA and re-referencing data
542 to the average of both mastoid electrodes, data were segmented between -1000 to 4000ms
543 around the pinch onset. We then performed a Morlet wavelet analysis to investigate
544 sensorimotor alpha and beta activity locked to pinch onset. This analysis was performed on
545 every trial for frequencies from 5 to 40 Hz with the number of cycles increasing linearly from
546 4 to 10. Thus, a wavelet at 10 Hz was 4.9 cycles long, had a temporal resolution of 0.10 s and
547 a spectral resolution of 4.85 Hz. We then calculated the average time-frequency activity for
548 each cardiac phase per subject.
549

550 Statistics

551 We statistically tested the two-condition comparisons of TEPs, HEPs, EMG linear envelope
552 and sensorimotor oscillations using cluster-based permutation *t*-tests as implemented in the
553 FieldTrip toolbox [48]. Statistical analysis of TEP activity during systole and diastole were
554 conducted over a set of electrodes over (C4, CP4, C6, CP6) between 15-60 ms. Pre- and post-
555 TMS changes in heart rate for stimulation during systole and diastole were evaluated using
556 within-subject ANOVAs (ezANOVA function in R [49,50]), in which heart rate was the dependent
557 variable and time (pre-TMS, TMS, post-TMS) as well as cardiac phase (systole, diastole) were
558 independent variables. For statistical testing of HEP activity across the changes in motor
559 excitability, we first sorted single trials according to their MEP amplitudes and split them into
560 three equal bins for each participant. For the weakest and strongest MEP bins, we then
561 contrasted prestimulus HEP amplitudes between 296 – 400 ms over a cluster of electrodes
562 (FC2, Cz, C4, CP1, CP2, Pz, P4, C1, C2, CPz, CP4, P1, P2), in which we previously observed
563 significant modulations of HEP preceding somatosensory processes [10,12].

564

565 During the motor task, the statistical analysis focused on the first second of the muscle
566 contraction following the pinch onset since cardiac effect are expected to be transient and
567 last for one cardiac cycle. Therefore, statistical analysis of the EMG envelope during systole
568 and diastole were conducted between 0-1000 ms. During the same time window,
569 sensorimotor oscillations were compared in the range of 8-30 Hz over a set of electrodes over
570 sensorimotor regions (C4, CP4, C6, CP6) using cluster statistics, in order to account for
571 multiple comparisons in the time, channel and frequency domain.

572

573 Repeated measures correlation coefficient was calculated to test the changes in the heart
574 rate across the motor excitability levels by using 'rmcorr' function [51] in R (v 1.3.1093).

575

576 Linear-Mixed-Effects Model

577 To test the relationship between MEP amplitudes and the distance from the previous
578 heartbeat, linear-mixed-effects models were fitted on the single-trial level. First, we
579 hierarchically compared a null model, which assumes no relationship (MEP~ (1 | subject) to a
580 model which assumes a linear relationship between MEP amplitudes and the distance (MEP
581 ~ distance + (1 | subject)). Then, we compared this linear model to a second-degree

582 polynomial model (MEP)~ distance + distance^2+ (1 | subject). In these models, we used the
583 natural logarithmic transformation of MEP amplitudes.
584
585 **Data availability**
586 The datasets generated during the current study are available from the corresponding author
587 on reasonable request. Due to a lack of explicit consent on the part of the participants to data
588 sharing, structural MRI and EEG data cannot be shared publicly. Such data can only be shared
589 if data privacy can be guaranteed according to the rules of the European General Data
590 Protection Regulation.
591
592 **Author contributions**
593 E.A., T.S., M.E., A.V., and V.N. designed the experiment, E.A. acquired the data. E.A., T.S., and
594 V.N. analyzed the data. E.A., T.S, A.V., and V.N. wrote the paper.
595
596 **Competing Interests**
597 The authors declare that they have no competing financial interests.
598
599 **References**

600 1. Allen, M., Frank, D., Samuel Schwarzkopf, D., Fardo, F., Winston, J. S., Hauser, T. U. &
601 Rees, G. Unexpected arousal modulates the influence of sensory noise on confidence.
602 *Elife* **5,** (2016).
603 2. Critchley, H. D. & Garfinkel, S. N. The influence of physiological signals on cognition.
604 *Curr. Opin. Behav. Sci.* **19,** 13–18 (2018).
605 3. Azzalini, D., Rebollo, I. & Tallon-Baudry, C. Visceral Signals Shape Brain Dynamics and
606 Cognition. *Trends Cogn. Sci.* **23,** 488–509 (2019).
607 4. Perl, O., Ravia, A., Rubinson, M., Eisen, A., Soroka, T., Mor, N., Secundo, L. & Sobel, N.
608 Human non-olfactory cognition phase-locked with inhalation. *Nat. Hum. Behav. 2019*
609 *35* **3,** 501–512 (2019).
610 5. Park, H.-D., Barnoud, C., Trang, H., Kannape, O. A., Schaller, K. & Blanke, O. Breathing
611 is coupled with voluntary action and the cortical readiness potential. *Nat. Commun.*
612 *2020 111* **11,** 1–8 (2020).
613 6. Sandman, C. A., McCanne, T. R., Kaiser, D. N. & Diamond, B. Heart rate and cardiac

614 phase influences on visual perception. *J. Comp. Physiol. Psychol.* **91,** 189–202 (1977).
615 7. Saxon, S. A. Detection of near threshold signals during four phases of cardiac cycle.
616 *Ala. J. Med. Sci.* **7,** 427–30 (1970).
617 8. Van Elk, M., Lenggenhager, B., Heydrich, L. & Blanke, O. Suppression of the auditory
618 N1-component for heartbeat-related sounds reflects interoceptive predictive coding.
619 *Biol. Psychol.* **99,** 172–182 (2014).
620 9. Wilkinson, M., McIntyre, D. & Edwards, L. Electrocutaneous pain thresholds are
621 higher during systole than diastole. *Biol. Psychol.* **94,** 71–73 (2013).
622 10. Al, E., Iliopoulos, F., Forschack, N., Nierhaus, T., Grund, M., Motyka, P., Gaebler, M.,
623 Nikulin, V. V. & Villringer, A. Heart-brain interactions shape somatosensory
624 perception and evoked potentials. *Proc. Natl. Acad. Sci. U. S. A.* **117,** 10575–10584
625 (2020).
626 11. Motyka, P., Grund, M., Forschack, N., Al, E., Villringer, A. & Gaebler, M. Interactions
627 between cardiac activity and conscious somatosensory perception. *Psychophysiology*
628 e13424 (2019).
629 12. Al, E., Iliopoulos, F., Nikulin, V. V. & Villringer, A. Heartbeat and somatosensory
630 perception. *Neuroimage* **238,** 118247 (2021).
631 13. Duschek, S., Werner, N. S. & Paso, G. A. R. del. The behavioral impact of baroreflex
632 function: A review. *Psychophysiology* **50,** 1183–1193 (2013).
633 14. Kunzendorf, S., Klotzsche, F., Akbal, M., Villringer, A., Ohl, S. & Gaebler, M. Active
634 information sampling varies across the cardiac cycle. *Psychophysiology* **56,** 1–16
635 (2019).
636 15. Galvez-Pol, A., McConnell, R. & Kilner, J. M. Active sampling in visual search is coupled
637 to the cardiac cycle. *Cognition* **196,** (2020).
638 16. Ohl, S., Wohltat, C., Kliegl, R., Pollatos, O. & Engbert, R. Microsaccades are coupled to
639 heartbeat. *J. Neurosci.* **36,** 1237–1241 (2016).
640 17. Konttinen, N., Mets, T., Lyytinen, H. & Paananen, M. Timing of triggering in relation to
641 the cardiac cycle in nonelite rifle shooters. *Res. Q. Exerc. Sport* **74,** 395–400 (2003).
642 18. Park, H.-D., Correia, S., Ducorps, A. & Tallon-Baudry, C. Spontaneous fluctuations in
643 neural responses to heartbeats predict visual detection. *Nat. Neurosci.* **17,** 612–618
644 (2014).
645 19. Bianchini, E., Mancuso, M., Zampogna, A., Guerra, A. & Suppa, A. Cardiac cycle does

646 not affect motor evoked potential variability: A real-time EKG-EMG study. *Brain*
647 *Stimul. Basic, Transl. Clin. Res. Neuromodulation* **14,** 170–172 (2021).
648 20. Ellaway, P. H., Davey, N. J., Maskill, D. W., Rawlinson, S. R., Lewis, H. S. & Anissimova,
649 N. P. Variability in the amplitude of skeletal muscle responses to magnetic stimulation
650 of the motor cortex in man. *Electroencephalogr. Clin. Neurophysiol. Mot. Control* **109,**
651 104–113 (1998).
652 21. Otsuru, N., Miyaguchi, S., Kojima, S., Yamashiro, K., Sato, D., Yokota, H., Saito, K.,
653 Inukai, Y. & Onishi, H. Timing of Modulation of Corticospinal Excitability by Heartbeat
654 Differs with Interoceptive Accuracy. *Neuroscience* **433,** 156–162 (2020).
655 22. Zhong, X., Meyer, C. H., Schlesinger, D. J., Sheehan, J. P., Epstein, F. H., Larner, J. M.,
656 Benedict, S. H., Read, P. W., Sheng, K. & Cai, J. Tracking brain motion during the
657 cardiac cycle using spiral cine-DENSE MRI. *Med. Phys.* **36,** 3413–3419 (2009).
658 23. Wagshul, M. E., Eide, P. K. & Madsen, J. R. The pulsating brain: A review of
659 experimental and clinical studies of intracranial pulsatility. *Fluids Barriers CNS* **8,** 1–23
660 (2011).
661 24. Pfurtscheller, G., Stancak, A., Neuper, C. & Neuper, C. Event-related synchronization (
662 ERS) in the alpha band -an electrophysiological correlate of cortical idling: A review.
663 *Int. J. Psychophysiol.* **24,** 39–46 (1996).
664 25. Pfurtscheller, G. & Lopes da Silva, F. H. Event-related EEG/MEG synchronization and
665 desynchronization: basic principles. *Clin. Neurophysiol.* **110,** 1842–1857 (1999).
666 26. Allen, M., Levy, A., Parr, T. & Friston, K. J. In the Body's Eye: The Computational
667 Anatomy of Interoceptive Inference. *bioRxiv* 603928 (2019). doi:10.1101/603928
668 27. Milne, R. J., Aniss, A. M., Kay, N. E. & Gandevia, S. C. Reduction in perceived intensity
669 of cutaneous stimuli during movement: a quantitative study. *Exp. brain Res.* **70,** 569–
670 576 (1988).
671 28. Starr, A. & Cohen, L. G. 'Gating' of somatosensory evoked potentials begins before
672 the onset of voluntary movement in man. *Brain Res.* **348,** 183–186 (1985).
673 29. Seki, K. & Fetz, E. E. Gating of Sensory Input at Spinal and Cortical Levels during
674 Preparation and Execution of Voluntary Movement. *J. Neurosci.* **32,** 890 (2012).
675 30. Blumberger, D. M., Vila-Rodriguez, F., Thorpe, K. E., Feffer, K., Noda, Y., Giacobbe, P.,
676 Knyahnytska, Y., Kennedy, S. H., Lam, R. W., Daskalakis, Z. J. & Downar, J.
677 Effectiveness of theta burst versus high-frequency repetitive transcranial magnetic

stimulation in patients with depression (THREE-D): a randomised non-inferiority trial. *Lancet* **391,** 1683–1692 (2018).

31. Johansen-Berg, H., Rushworth, M. F., Bogdanovic, M. D., Kischka, U., Wimalaratna, S. & Matthews, P. M. The role of ipsilateral premotor cortex in hand movement after stroke. *Proc. Natl. Acad. Sci. U. S. A.* **99,** 14518–14523 (2002).

32. Udupa, K., Sathyaprabha, T. N., Thirthalli, J., Kishore, K. R., Raju, T. R. & Gangadhar, B. N. Modulation of cardiac autonomic functions in patients with major depression treated with repetitive transcranial magnetic stimulation. *J. Affect. Disord.* **104,** 231–236 (2007).

33. Iseger, T. A., Padberg, F., Kenemans, J. L., Gevirtz, R. & Arns, M. Neuro-Cardiac-Guided TMS (NCG-TMS): Probing DLPFC-sgACC-vagus nerve connectivity using heart rate – First results. *Brain Stimul.* **10,** 1006–1008 (2017).

34. Kaur, M., Michael, J. A., Hoy, K. E., Fitzgibbon, B. M., Ross, M. S., Iseger, T. A., Arns, M., Hudaib, A.-R. & Fitzgerald, P. B. Investigating high- and low-frequency neuro-cardiac-guided TMS for probing the frontal vagal pathway. *Brain Stimul. Basic, Transl. Clin. Res. Neuromodulation* **13,** 931–938 (2020).

35. Luft, C. D. B. & Bhattacharya, J. Aroused with heart: Modulation of heartbeat evoked potential by arousal induction and its oscillatory correlates. *Sci. Rep.* **5,** 1–11 (2015).

36. Löfberg, O., Julkunen, P., Pääkkönen, A. & Karhu, J. The auditory-evoked arousal modulates motor cortex excitability. *Neuroscience* **274,** 403–408 (2014).

37. Azarbarzin, A., Ostrowski, M., Hanly, P. & Younes, M. Relationship between arousal intensity and heart rate response to arousal. *Sleep* **37,** 645–653 (2014).

38. Oldfield, R. C. The assessment and analysis of handedness: The Edinburgh inventory. *Neuropsychologia* **9,** 97–113 (1971).

39. Nikouline, V., Ruohonen, J. & Ilmoniemi, R. J. The role of the coil click in TMS assessed with simultaneous EEG. *Clin. Neurophysiol.* **110,** 1325–1328 (1999).

40. Vázquez-Seisdedos, C. R., Neto, J. E., Marañón Reyes, E. J., Klautau, A. & Limão de Oliveira, R. C. New approach for T-wave end detection on electrocardiogram: performance in noisy conditions. *Biomed. Eng. Online* **10,** 77 (2011).

41. Hyvärinen, A. Fast and robust fixed-point algorithms for independent component analysis. *IEEE Trans. Neural Networks* **10,** 626–634 (1999).

42. Harquel, S., Bacle, T., Beynel, L., Marendaz, C., Chauvin, A. & David, O. Mapping

710 dynamical properties of cortical microcircuits using robotized TMS and EEG: Towards
711 functional cytoarchitectonics. *Neuroimage* **135,** 115–124 (2016).
712 43. Tadel, F., Baillet, S., Mosher, J. C., Pantazis, D. & Leahy, R. M. Brainstorm: A user-
713 friendly application for MEG/EEG analysis. *Comput. Intell. Neurosci.* **2011,** (2011).
714 44. Kybic, J., Clerc, M., Abboud, T., Faugeras, O., Keriven, R. & Papadopoulo, T. A common
715 formalism for the Integral formulations of the forward EEG problem. *IEEE Trans. Med.*
716 *Imaging* **24,** 12–28 (2005).
717 45. Gramfort, A., Papadopoulo, T., Olivi, E. & Clerc, M. OpenMEEG: opensource software
718 for quasistatic bioelectromagnetics. *Biomed. Eng. Online* **9,** 45 (2010).
719 46. Fonov, V., Evans, A., McKinstry, R., Almli, C. & Collins, D. Unbiased nonlinear average
720 age-appropriate brain templates from birth to adulthood. *Neuroimage* **47,** S102
721 (2009).
722 47. Winter, D. A. Biomechanics and Motor Control of Human Movement: Fourth Edition.
723 *Biomech. Mot. Control Hum. Mov. Fourth Ed.* 1–370 (2009).
724 48. Oostenveld, R., Fries, P., Maris, E. & Schoffelen, J.-M. FieldTrip: Open Source Software
725 for Advanced Analysis of MEG, EEG, and Invasive Electrophysiological Data. *Comput.*
726 *Intell. Neurosci.* **2011,** 1–9 (2011).
727 49. Lawrence, M. ez: Easy Analysis and Visualization of Factorial Experiments. (2016). at
728 <https://cran.r-project.org/package=ez>
729 50. R Development Core Team. R: A Language and Environment for Statistical Computing.
730 (2021).
731 51. Bakdash, J. & Marusich, L. rmcorr: Repeated Measures Correlation. (2021). at
732 <https://cran.r-project.org/package=rmcorr>
733 52. Morey, R. D. Confidence Intervals from Normalized Data: A correction to Cousineau
734 (2005). *Tutor. Quant. Methods Psychol.* **4,** 61–64 (2008).
735

Supplementary Files

This is a list of supplementary files associated with this preprint. Click to download.

- SupplementaryFiguresTMSEEG.pdf